

Synthesis and Characterization of Core-Shell NiO@Al₂O₃ with High Ni/Al Ratio and High Calcination Temperature

Intan Clarissa Sophiana^{1,*}, Ibnu Maulana Hidayatullah¹, Fatimah Azizah Riyadi^{1,*}

¹Department of Chemical Engineering, Faculty of Engineering, Universitas Indonesia, Depok 16424, Indonesia

*Correspondence: intan.clarissa@ui.ac.id, fatimah.azizah@ui.ac.id

<https://doi.org/10.37934/jrnn.9.1.3541>

ABSTRACT

Nanomaterials have made significant advancements in various applications, particularly in the field of catalysis. The limited lifespan of nickel-based catalysts due to sintering at high temperatures has presented a challenge that requires innovative solutions. This research focuses on the synthesis and characterization of core-shell materials designed to protect nickel from sintering occurring at temperatures around 600°C. NiO@Al₂O₃ samples were synthesized using the chemical reduction method and aluminum isopropoxide hydrolysis, with variations in the nickel-to-alumina ratio during calcination at 800°C. The samples were characterized using XRD and N₂ adsorption-desorption to assess crystallinity, crystallite size, surface area, pore diameter, and pore volume. The results demonstrate the successful formation of NiO encapsulated within alumina (NiO@Al₂O₃), minimizing nickel agglomeration and aggregation, as indicated by the conducted characterizations. These findings enable the development of catalysts with high stability and extended lifespans for various high-temperature nickel-based catalytic reactions.

Keywords:

Nanomaterial, core-shell, NiO@Al₂O₃, XRD, BET, characterization

Received: 23 Aug. 2023

Revised: 10 Okt. 2023

Accepted: 29 Nov. 2023

Published: 7 Dec. 2023

1. Introduction

In the context of current advances in nanomaterial technology, the development of efficient catalysts for high-temperature catalytic reactions has become a primary focus in the field of catalytic chemistry. Nanomaterial technology enables the manipulation of material structure and properties at the nanoscale, allowing for a significant enhancement in catalyst performance, particularly under extreme operating conditions such as high temperatures [1].

High temperatures facilitate chemical reactions with accelerated kinetics, leading to improved desired product yields. Nickel (Ni), owing to its unique chemical and physical properties, has

garnered attention as a catalytic material. Nickel serves as a catalyst in various reactions, encompassing dry reforming, steam reforming, and various others [2-4].

Nickel catalysts have proven to be an attractive choice in various industrial applications due to their cost-effectiveness and abundance compared to noble metals. However, a primary challenge faced is maintaining catalyst stability at high temperatures, as thermal degradation, known as sintering, occurs typically at temperatures around 700-800°C [5,6]. Sintered nickel catalysts lead to the agglomeration and aggregation of nickel particles, potentially obstructing catalyst pores and resulting in diminished catalyst performance. Consequently, Ni-based catalysts necessitate modification to enhance their efficacy [7].

Ongoing research endeavors by several researchers focus on the development of catalysts with a core-shell morphology for reforming processes [8-11]. This morphology involves encapsulating the active metal center of the catalyst with a porous shell. Such encapsulation of the nickel surface, the active center of the catalyst, within porous materials, serves to restrict the agglomeration and aggregation of nickel particles while safeguarding the catalyst's active center [12,13]. The core-shell morphology is achieved by forming active metal particles as 'nuclei' and subsequently synthesizing porous material to create a 'shell' that envelops the core as a protective shield [14].

The use of silica as a shell in catalysts with core-shell morphology aids in stabilizing the active nickel center against sintering at high temperatures [15]. However, research involving alumina as a shell on a catalyst is presently less widely reported, despite alumina being better suited for reactions involving acidic gases such as CO₂ and CH₄. Researchers who have developed such catalysts include Baktash *et al.*, [5] and Huang *et al.*, [16], employing methods like Atomic Layer Deposition (ALD) and inverse microemulsion. Their findings indicate that the Ni@Al₂O₃ catalyst exhibits greater stability compared to the Ni/Al₂O₃ catalyst.

This study aims to investigate the influence of nickel and alumina composition on the characterization of nickel-based core-shell catalysts. It is anticipated that this approach will pave the way for the development of more efficient and durable nickel-based core-shell catalysts for various high-temperature catalytic reactions. The anticipated outcomes of this research endeavor are poised to contribute significantly to advancements in the field of catalysis and industrial process technology.

2. Materials and Methods

2.1 Materials

Nickel chloride hexahydrate (NiCl₂·6H₂O, > 99.9%, Merck), sodium borohydride (NaBH₄, > 98%, Merck), polyvinylpyrrolidone ((C₆H₉NO)_n, > 99%, Merck), cetil trimethyl ammonium bromide (C₁₉H₄₂BrN ≥ 98%, Sigma-Aldrich), aluminum isopropoxide (C₉H₂₁AlO₃, > 99.9%, Merck), ammonium nitrate (NH₄OH, 25%, Merck), and ethanol pro analysis (Ce(NO₃)₃·6H₂O, > 99.5%, Merck) were used in this study. Demineralized water was used throughout the whole synthesis. All materials were used without further purification.

2.2 Preparation of Samples

The synthesis of NiO@Al₂O₃ was conducted by varying the quantities of alumina derived from aluminium isopropoxide (AIP) as a shell of materials to nickel nanoparticles as a core of materials.

2.2.1 Synthesis of Nickel Nanoparticles

Initially, 3.2 grams of $\text{Ni}(\text{Cl})_2 \cdot 6\text{H}_2\text{O}$ solids were dissolved in 600 mL of demineralized water, and then 0.32 grams of PVP were added as a stabilizer and stirred until homogenized. The solution was subjected to sonication using an ultrasonicator probe at 25°C and atmospheric pressure. Following the ultrasonication step, 160 mL of 0.01 M NaBH_4 was introduced into the sample using a syringe pump, with a flow rate of 150 mL per hour. The mixture was stirred using a magnetic stirrer at 600 rpm in a nitrogen atmosphere with a flow rate of 2 mL per second. Additionally, an aging process was conducted for approximately 1 hour at room temperature (25°C) and pressure, with continuous stirring at 600 rpm in a nitrogen atmosphere. Then, the separation and washing of nickel nanoparticles were carried out using a centrifuge operating at 20,000 rpm for 10 minutes. The resulting nickel nanoparticles were subsequently oven-dried at 100°C and atmospheric pressure for 12 hours.

2.2.2 Synthesis of $\text{NiO}@\text{Al}_2\text{O}_3$

A solid mass of 2.4 g of nickel nanoparticles, with or without the addition of synthesized promoters, was dispersed in 600 mL of ethanol and subjected to ultrasonication for 30 minutes. Following ultrasonication, AIP and cetyl trimethyl ammonium bromide (CTAB) were introduced into the suspension, which was then stirred at 600 rpm and heated to 45°C for 1 hour. Subsequently, 60 mL of demineralized water was added to the suspension while stirring, and the mixture was allowed to stand for 24 hours at room temperature to facilitate the aging process. This resulted in the formation of nickel nanoparticles coated with alumina, which were obtained in the form of sediment. The solution was separated using a centrifuge at 20,000 rpm, and the sample was then washed and dried at 100°C for 12 hours. Finally, the samples were subjected to calcination at 800°C for 6 hours. The formed samples have nickel compositions of 81% by weight (81% $\text{NiO}@\text{Al}_2\text{O}_3$) and 58% by weight (58% $\text{NiO}@\text{Al}_2\text{O}_3$).

2.3 Characterization of Samples

2.3.1 X-ray diffraction (XRD)

The crystallinity of the sample was determined using XRD. XRD measurements of the samples were conducted with a Philips X'Pert MDR diffractometer equipped with a Cu anode tube capable of generating $\text{Cu-K}\alpha$ X-rays at 1.5405 Å, using a scan rate of 20° per minute. The sample was positioned in the diffractometer cell and irradiated with X-rays emitted by a Cu metal source. Diffraction data were collected over the 2θ angle range of 5-90° at a scan rate of 4° per minute. The resulting diffractogram represents the relationship between intensity and the diffraction angle 2θ . The crystal size of the metal was determined using the Scherrer equation.

2.3.2 N_2 adsorption-desorption

The specific surface area of the sample was measured using the Brunauer–Emmett–Teller (BET) isotherm method, which relies on nitrogen adsorption-desorption. The measurements were performed with the Quantachrome NOVA 1000 Gas Sorption Analyzer instrument. To initiate the analysis, the solid powder under examination was placed in a sample cell for weighing. Subsequently, the sample cell was positioned in an outgasser, where outgassing was conducted to remove water molecules and impurity gases adhering to the sample surface. This outgassing process was performed

isothermally at 250°C for a duration of 2 hours. Then, the sample was cooled to room temperature (25°C). The sample cell was then transferred to the Gas Sorption Analyzer for further analysis. The distribution of pore diameters was then determined using the Barrett-Joyner-Halenda (BJH) method.

3. Results and Discussion

3.1 Crystal Structure and Crystallite Size of NiO@Al₂O₃

3.1.1 Crystal phase and crystallinity of NiO@Al₂O₃

Figure 1 illustrates the peaks observed in all samples containing NiO components. It is evident that each sample exhibits five distinct NiO peaks at different 2θ values: 37.28°, 43.30°, 62.92°, 75.45°, and 79.39°, which correspond to the (1 1 1), (2 0 0), (2 2 0), (3 1 1), and (2 2 2) crystal planes, respectively, as defined in the JCPDS 73-1523 database. These peaks are indicative of a cubic crystalline phase. In contrast, the Al₂O₃ component does not exhibit clear peaks due to the formation of an amorphous phase caused by insufficient aging time during the synthesis process. With a higher nickel composition, additional peaks emerge, albeit with lower intensity. Some of these newly formed peaks are partially suspected to be associated with NiAl₂O₄ spinel components, while others represent unknown phases.

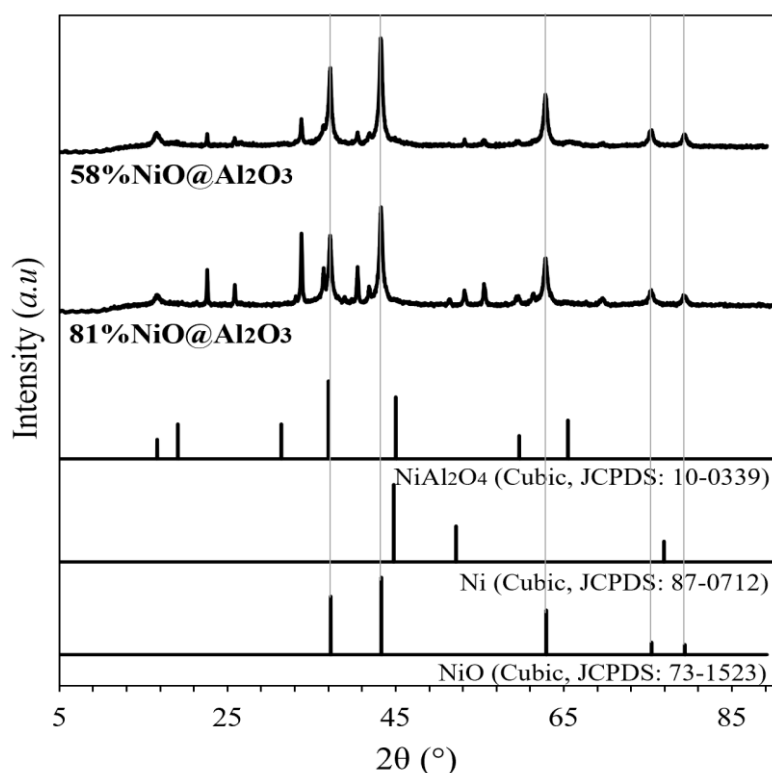


Fig. 1. XRD results of 58%NiO@Al₂O₃ and 81%NiO@Al₂O₃

3.1.2 Crystallite size of NiO@Al₂O₃

The average crystallite size of NiO was determined using the Scherrer equation. This crystallite size serves as a key parameter for understanding the behavior of the nickel component as the nickel composition of the sample increases. Overall, the increase in nickel content does not significantly influence the crystallite size, as demonstrated in Table 1. The 81%NiO@Al₂O₃ and 58%NiO@Al₂O₃

samples exhibit NiO crystallite sizes within a similar range, typically ranging from 12 to 13 nm. This occurrence can be attributed to the successful formation of NiO encapsulated within alumina (NiO@Al₂O₃), where the alumina effectively shields the nickel oxide from coalescing with other nickel oxide particles during sintering processes.

Table 1. Physical properties of the samples

Sample	Crystallite size of NiO (nm)	Surface Area (m ² g ⁻¹)	Pore Diameter (nm)	Total pore volume (cm ³ g ⁻¹)
81%NiO@Al ₂ O ₃	12.56	62	20.0	0.309
58%NiO@Al ₂ O ₃	12.76	117	15.7	0.459

3.2 N₂ Adsorption-Desorption

In Figure 2(A), the synthesized samples of both 81%NiO@Al₂O₃ and 58%NiO@Al₂O₃ are classified as type IV isotherms, following the mesoporous solids classification. This isotherm classification describes monolayer-multilayer adsorption on the mesoporous walls. Mesoporous solids are characterized by pore diameters ranging from 2 to 50 nm. In this phenomenon, a hysteresis loop is observed due to capillary condensation within the mesoporous samples. The hysteresis loop type for these samples is categorized as type H3, which does not exhibit limiting adsorption at high P/P₀. Desorption in this type includes regions associated with hysteresis closure due to the effect of surface tension forces.

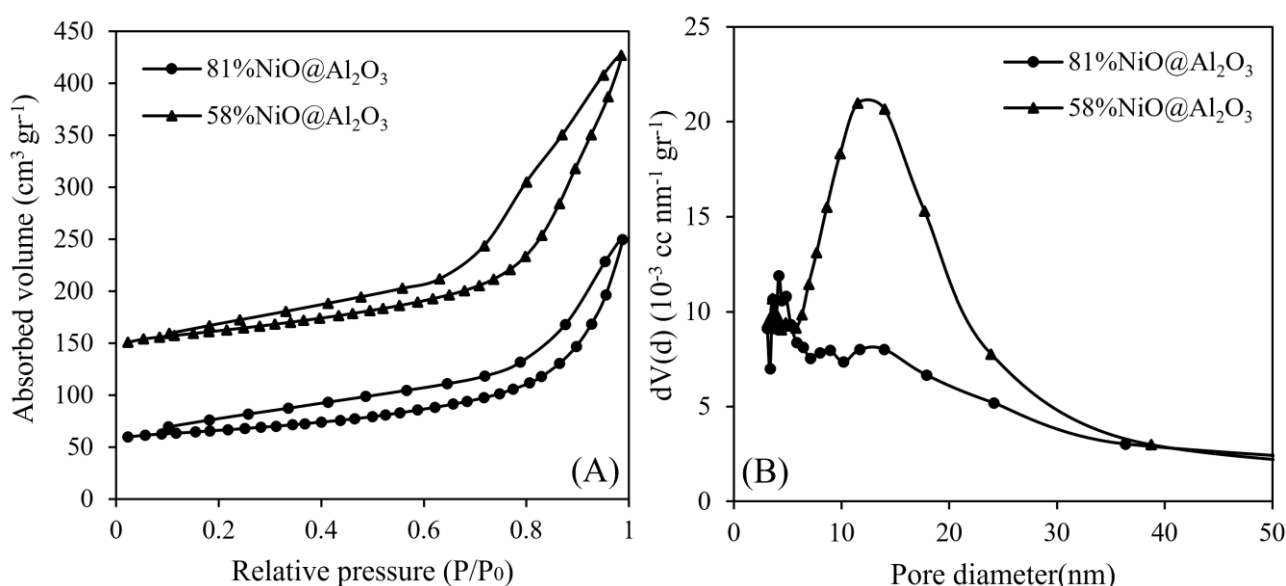


Fig. 2. Nitrogen adsorption–desorption of sample: (A) Absorbed volume, and (B) Pore diameter of 58%NiO@Al₂O₃ and 81%NiO@Al₂O₃

In Table 1, the surface area of samples with a 58% by-weight nickel composition can be observed to reach 117 m² g⁻¹, with a pore volume of 15.7 nm and 0.459 cm³ g⁻¹. Conversely, in a sample with the 81% nickel composition, the surface area decreases by approximately 45% to 62 m² g⁻¹, with a corresponding 33% reduction in pore volume to 0.309 cm³ g⁻¹. Analysing the pore distribution, the 58%NiO@Al₂O₃ sample reveals a relatively narrow distribution with an average pore diameter of approximately 15.7 nm. In contrast, the 81%NiO@Al₂O₃ sample exhibits a broader range of pore

distribution, with an increased average pore diameter of 20 nm. This is attributed to the sintering phenomenon occurring in alumina at 800°C, which enlarges the pore diameter and consequently reduces the surface area of the sample.

4. Conclusions

NiO@Al₂O₃ was synthesized using a chemical reduction method and AIP hydrolysis with variations in the nickel-alumina ratio. Both 58% NiO@Al₂O₃ and 81% NiO@Al₂O₃ contain NiO components that exhibit a crystalline structure, as confirmed by JCPDS 73-152 analysis, while the alumina components are amorphous based on XRD analysis. The differences in nickel composition in the samples do not affect the range of NiO crystallite sizes following calcination at 800°C. This indicates the successful formation of NiO encapsulated with alumina (NiO@Al₂O₃), where alumina can protect nickel oxide from agglomerating with other nickel oxides at high temperatures. However, from the nitrogen adsorption-desorption analysis, the surface area and pore volume of samples containing higher nickel content are smaller compared to samples with lower nickel content. This could be a result of the sintering phenomenon that occurs in alumina at 800°C, which enlarges the pore diameter and consequently reduces the surface area of the samples. Nevertheless, despite alumina experiencing sintering, both the 81%-weight and 58%-weight nickel oxide compositions remain optimal for protecting nickel oxide as the core against sintering, preventing nickel oxide particles from agglomerating and forming larger particles.

Funding

This research was funded by the Ministry of Education, Culture, Research, and Technology (KEMENDIKBUDRISTEK) Republic of Indonesia under the Program Magister Doktor untuk Sarjana Unggul (PMDSU) and World Class University (WCU) for research funding support.

Acknowledgement

We would like to express our sincere gratitude to Prof. Norizaku Nishiyama of the Chemical Engineering Department at Osaka University for facilitating the characterization of N₂ adsorption-desorption in this study, Prof. Yogi Wibisono Budhi from the Department of Chemical Engineering at Institut Teknologi Bandung (ITB) for enabling the XRD analysis, and Prof. Ferry Iskandar from the Department of Physics at the ITB for providing access to the ultrasonic equipment.

References

1. Abdulrasheed, Abdulrahman, Aishah Abdul Jalil, Yahya Gambo, Maryam Ibrahim, Hambali Umar Hambali, and Muhamed Yusuf Shahul Hamid. "A review on catalyst development for dry reforming of methane to syngas: Recent advances." *Renewable and Sustainable Energy Reviews* 108 (2019): 175-193. <https://doi.org/10.1016/j.rser.2019.03.054>
2. Sophiana, Intan Clarissa, Ferry Iskandar, Hary Devianto, Norikazu Nishiyama, and Yogi Wibisono Budhi. "Coke-Resistant Ni/CeZrO₂ catalysts for dry reforming of methane to produce Hydrogen-Rich syngas." *Nanomaterials* 12, no. 9 (2022): 1556. <https://doi.org/10.3390/nano12091556>
3. Nisa, K. S., V. Suendo, I. C. Sophiana, H. Susanto, A. Kusumaatmaja, N. Nishiyama, and Y. W. Budhi. "Effect of base promoter on activity of MCM-41-supported nickel catalyst for hydrogen production via dry reforming of methane." *International Journal of Hydrogen Energy* 47, no. 55 (2022): 23201-23212. <https://doi.org/10.1016/j.ijhydene.2022.05.081>

4. Budhi, Yogi Wibisono, Fitri Az Zahra, Wulan Reyhana, Salma Liska, Intan Clarissa Sophiana, Elvi Restiawaty, Manabu Miyamoto, Shigeyuki Uemiya, and Norikazu Nishiyama. "Enhancing the catalytic performance and coke reduction using low-cost Ni-based promoted catalyst for hydrogen production." *Journal of Industrial and Engineering Chemistry* (2023). <https://doi.org/10.1016/j.jiec.2023.08.013>
5. Baktash, Elham, Patrick Littlewood, Reinhard Schomäcker, Arne Thomas, and Peter C. Stair. "Alumina coated nickel nanoparticles as a highly active catalyst for dry reforming of methane." *Applied Catalysis B: Environmental* 179 (2015): 122-127. <https://doi.org/10.1016/j.apcatb.2015.05.018>
6. Sehested, Jens, Johannes AP Gelten, and Stig Helveg. "Sintering of nickel catalysts: Effects of time, atmosphere, temperature, nickel-carrier interactions, and dopants." *Applied Catalysis A: General* 309, no. 2 (2006): 237-246. <https://doi.org/10.1016/j.apcata.2006.05.017>
7. Zhang, Guojie, Jiwei Liu, Ying Xu, and Yinghui Sun. "A review of CH₄CO₂ reforming to synthesis gas over Ni-based catalysts in recent years (2010–2017)." *International Journal of Hydrogen Energy* 43, no. 32 (2018): 15030-15054. <https://doi.org/10.1016/j.ijhydene.2018.06.091>
8. Li, Ziwei, Zhigang Wang, and Sibudjing Kawi. "Sintering and coke resistant core/yolk shell catalyst for hydrocarbon reforming." *ChemCatChem* 11, no. 1 (2019): 202-224. <https://doi.org/10.1002/cctc.201801266>
9. Ghosh Chaudhuri, Rajib, and Santanu Paria. "Core/shell nanoparticles: classes, properties, synthesis mechanisms, characterization, and applications." *Chemical reviews* 112, no. 4 (2012): 2373-2433. <https://doi.org/10.1021/cr100449n>
10. Dai, Chengyi, Shaohua Zhang, Anfeng Zhang, Chunshan Song, Chuan Shi, and Xinwen Guo. "Hollow zeolite encapsulated Ni–Pt bimetal for sintering and coking resistant dry reforming of methane." *Journal of Materials Chemistry A* 3, no. 32 (2015): 16461-16468. <https://doi.org/10.1039/C5TA03565A>
11. Pu, Jianglong, Katsuki Nishikado, Ningning Wang, Thanh Tung Nguyen, Tei Maki, and Eika W. Qian. "Core-shell nickel catalysts for the steam reforming of acetic acid." *Applied Catalysis B: Environmental* 224 (2018): 69-79. <https://doi.org/10.1016/j.apcatb.2017.09.058>
12. Jabbour, Karam, Pascale Massiani, Anne Davidson, Sandra Casale, and Nissrine El Hassan. "Ordered mesoporous "one-pot" synthesized Ni-Mg (Ca)-Al₂O₃ as effective and remarkably stable catalysts for combined steam and dry reforming of methane (CSDRM)." *Applied Catalysis B: Environmental* 201 (2017): 527-542. <https://doi.org/10.1016/j.apcatb.2016.08.009>
13. Zhang, Qiao, Ilkeun Lee, Ji Bong Joo, Francisco Zaera, and Yadong Yin. "Core-shell nanostructured catalysts." *Accounts of Chemical Research* 46, no. 8 (2013): 1816-1824. <https://doi.org/10.1021/ar300230s>
14. Almana, Noor, Somphonh Peter Phivilay, Paco Laveille, Mohamed N. Hedhili, Paolo Fornasiero, Kazuhiro Takanabe, and Jean-Marie Basset. "Design of a core-shell Pt–SiO₂ catalyst in a reverse microemulsion system: Distinctive kinetics on CO oxidation at low temperature." *Journal of catalysis* 340 (2016): 368-375. <https://doi.org/10.1016/j.jcat.2016.06.002>
15. Majewski, Artur J., Joseph Wood, and Waldemar Bujalski. "Nickel-silica core@ shell catalyst for methane reforming." *International Journal of Hydrogen Energy* 38, no. 34 (2013): 14531-14541. <https://doi.org/10.1016/j.ijhydene.2013.09.017>
16. Huang, Qiong, Xiuzhong Fang, Qinzheng Cheng, Qian Li, Xianglan Xu, Luoqi Xu, Wenming Liu, Zhixian Gao, Wufeng Zhou, and Xiang Wang. "Synthesis of a Highly Active and Stable Nickel-Embedded Alumina Catalyst for Methane Dry Reforming: On the Confinement Effects of Alumina Shells for Nickel Nanoparticles." *ChemCatChem* 9, no. 18 (2017): 3563-3571. <https://doi.org/10.1002/cctc.201700490>